# Catalytically inactive Gla-domainless factor Xa binds to TFPI and restores *ex vivo* coagulation in hemophilia plasma

*Atanur Ersayin,[1] Aline Thomas,[2] Landry Seyve,[1] Nicole Thielens,[3] Mathieu Castellan,[1] Raphaël Marlu,[1] Benoît Polack[1] and Marie-Claire Dagher[1]*

*[1]University of Grenoble Alpes, CNRS, CHU Grenoble Alpes, Grenoble INP, TIMC-IMAG, Institute of Engineering, University Grenoble Alpes; [2]University of Grenoble Alpes, CNRS, DPM, and [3]University of Grenoble Alpes, CEA, CNRS, IBS, Grenoble, France*

*AE and AT contributed equally to this work.*

*Correspondence: marie-claire.dagher@univ-grenoble-alpes.fr*
*doi:10.3324/haematol.2017.174037*

**Ersayin et al. Supplementary online material**

# Supplementary Methods

## Production of TFPI alpha and S195A GD-FXa

The optimized cDNA sequences were obtained from Genscript. The proteins were expressed in S2 cells (Drosophila Expression System, Life Technologies). GD-FXa was produced as a single polypeptide chain where the activation peptide was replaced by a linker containing a double furin cleavage site. An HPC4 tag (Protein C derived epitope) was present at the C-terminus. S2 cells were transfected with Freestyle Max Reagent (Life Technologies), and the supernatant was collected at day 6 post transfection. TFPI was purified on a SP-Sepharose column (GE Healthcare) and displayed 95% purity after this step. GD-FXa was very unstable and could not be purified. After cation exchange chromatography, the S195A GD-FXa protein was further purified on an anti-Protein C Affinity matrix (Roche). TFPI activity was checked by inhibition of FXa using the chromogenic substrate PNAPEP-1025 (Cryopep) and by binding to FXa by surface plasmon resonance. For S195A GD-FXa, correct processing at the furin cleavage site was confirmed by mass spectrometry analysis.

## Surface plasmon resonance

First, to assess the functionality of TFPI, increasing concentrations of FXa (Cryopep) were injected over TFPI covalently immobilized on a CM5 sensorchip (GE Healthcare). The kinetic constants were calculated using the Biaeval software (GE Healthcare) and the ratio of the dissociation and association rate constants yielded a $K_D$ of 2.2 nM. Immobilized TFPI was then used to measure the binding constants of plasma derived GD-FXa (Cryopep) or S195A GD-FXa.

## Thrombin generation assay

Thrombin generation was assayed in FVIII or FIX immuno-depleted plasmas and in plasmas from hemophilia A and B patients (Cryopep). One hemophilia A plasma with inhibitor (50 BU) was also assayed. Plasma was spiked with S195A GD-FXa or recombinant FVIII (Octocog alpha, Bayer Pharma) or plasma derived FIX (Cryopep) and thrombin generation was triggered by 1 pM tissue factor and 4 µM phospholipids (PPP-reagent low, Stago) in the presence of a fluorogenic substrate (FluCa kit, Diagnostica Stago). All assays were run in triplicates on a CAT fluorimeter (Stago). Thrombin generation was monitored after excitation at 390 nm and emission at 460 nm for 60 min at 37°C. The curves were fitted

using Thrombinoscope Software V5.0 (Stago). Controls were run with FX deficient plasmas and in the absence of tissue factor using MP-reagent Stago instead of PPP-reagent low (Stago).

### Molecular Dynamics

To characterize the effect of the S195A mutation on the molecular interactions of FXa with the K2 domain of TFPI, molecular dynamics calculations of the wild-type FXa/K2 and of the S195A FXa/K2 complexes were performed. These simulations were done with the CHARMM software (1, 2) using the CHARMM-36 parameters and topology sets including the CMAP correction (3); the total charge of the system was null so that no counter-ion was added.

The systems were fully solvated in a TIP3P (4) water box of 16 Å edge larger than the protein dimensions. The molecular systems totalize about 35000 atoms including about 4580 protein atoms.

Periodic boundary conditions were used to model the solvent. A minimization procedure was performed with decreasing harmonic forces on all the atoms, totalizing 3000 steps of steepest descent followed by 5000 steps of ABNR minimization without constraints. The structures were then subjected to a CPT molecular dynamics (5) (1 atm, 298 K). The molecular systems were annealed from 48 K to 298 K over a period of 20 ps and maintained at that temperature with velocity scaling. The non-bonding interactions were considered up to a cutoff of 14 Å, and smoothly zeroed between 12 Å and 14 Å using a shifting potential. Covalent bonds involving hydrogens were kept fixed using the SHAKE algorithm (6), thus allowing an integration time step of 2 fs. The systems were equilibrated for 10 ns and the production runs lasted 100 ns. The trend of the overall potential energy, root mean square deviations (RMSD) and gyration radius, indicate that the systems are well stabilized after 10 ns.

## Supplementary results

### The molecular interface along the dynamics

The hydrogen bond between S195$(O\gamma)_{FXa}$ and R15$(N)_{K2}$ that was present in the starting porcine trypsin-K2 complex (7), is not present in the wild-type FXa-K2 complex as the serine side-chain is hydrogen bonded to surrounding water molecules. As shown in Supplementary Figure 1, the R15$(N)_{K2}$ is stabilized by two strong and stable hydrogen bonds with respectively G193$(N)_{FXa}$ and S195$(N)_{FXa.}$ The hydrogen bond between G216$(N)_{FXa}$ and I13$(O)_{K2}$ is conserved throughout the dynamics. The $R15_{K2}$ side-chain extends in the specificity pocket with its guanidinium group forming a salt-bridge with the carboxylate group of $D189_{FXa}$, fully conserved along the trajectories. When compared to the porcine trypsin-K2 complex (7),

the very close neighborhood of K2 is conserved, except residue $S190_{Trypsin}$ which is an alanine in FXa. Thus, the hydrogen bond of $R15(NH1)_{K2}$ with the side-chain of residue 190 disappears whether the hydrogen bond between $R15(NH1)_{K2}$ and the $G219_{FXa}$ backbone oxygen is maintained. A hydrogen bond between the carboxamide nitrogen of $Q192_{FXa}$ and the $C14(O)_{K2}$ appears after 50 ns. The $S214(O\gamma)_{FXa}$ entertains a hydrogen bond with $D102(OD2)_{FXa}$ which is replaced after 50 ns by a hydrogen bond with $W215(NE)_{FXa}$. The distribution of the residual interaction energies between FXa residues and the K2 chain (see Supplementary Figure 2) shows that the mutation of S195 into an alanine does not perturb the interface between both proteins.

## Estimation of free energies of binding

Approximate free energies of binding of TFPI-K2 to the catalytic domain of wild-type and S195A FXa were calculated using the MMPBSA solvent continuum approximation (8) as follows.

The binding free energy can be approximated as:

$G = E - TS$

The internal energy terms can be assumed to be the same in the native complex and in the mutated one, so that E can be taken as $E_{vdw}$. Furthermore, we can assume that the entropic contribution cancels when one calculates the difference in binding free energies $\Delta\Delta G_{bind}$ between the wild-type and the mutated complexes. Thus,

$G = \lambda E_{vdw} + G_{elec} + \gamma G_{non\ polar} + \varepsilon$

$E_{vdw}$ is the standard Lennard-Jones term calculated with a quasi infinite cutoff (of 120.0 Å) for non-bonded interactions. The total electrostatic contribution to the binding free energy was calculated using the Poisson Boltzman equation, with the PBEQ solver. The protein dielectric constant was then taken as 4 and the solvent one as 80. The nonpolar contribution was estimated as a fraction of the surface accessible area (9), with $\gamma$=0.00542 kcal/mol.$Å^2$ and $\varepsilon = 0.92$. The different energy contributions were calculated for each snapshot every 1 ns along the trajectories and the averages (in kcal/mol) are presented in the following table.

| System | $\Delta E_{vdw}$ | $\Delta G_{elec}$ | $\Delta G_{non\ polar}$ | $\Delta G$ |
|---|---|---|---|---|
| Wild | -14.47 ± 1.73 | -15.52 ±2.49 | -9.24 ± 0.85 | -39.24 ± 2.25 |
| SA195 | -14.95 ±1.07 | -16.79 ±2.16 | -9.38 ±0.47 | -41.14 ± 2.39 |

Even though there is a rough approximation for the calculation of the free energies of binding by neglecting the solvation entropy, the $\Delta G$ values indicate that the S195A mutation does not perturb the affinity of TFPI-K2 for FXa.

## Supplementary figures

**Supplementary Figure 1: Model of the interaction between the catalytic domain of FXa and the K2 domain of TFPI.**

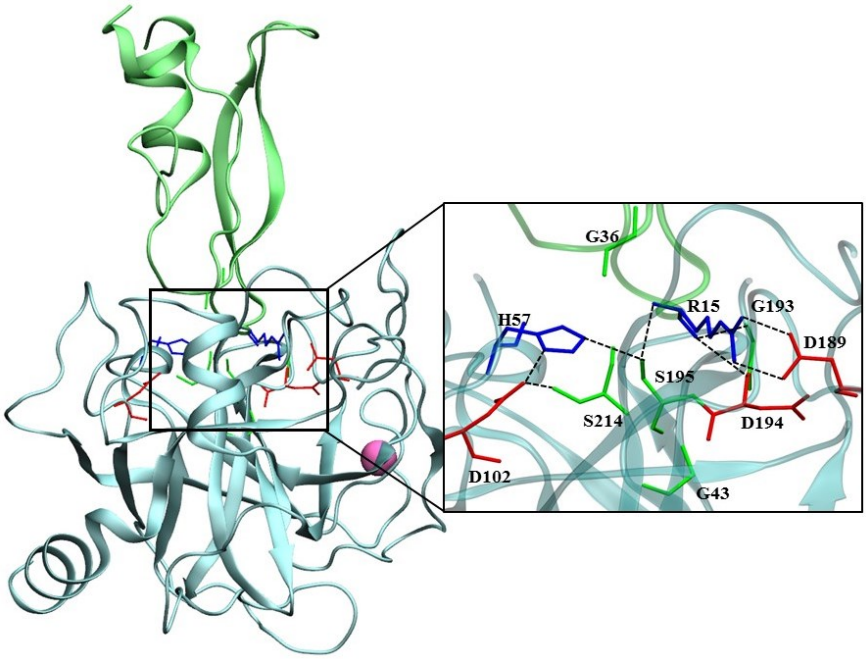


The catalytic domain of FXa and the K2 domain of TFPI are respectively drawn as cyan and green ribbons. The calcium ion is represented as a purple sphere. A zoom on the active site shows the insertion of $R15_{K2}$ within the FXa active site. The main hydrogen bonds stabilizing the interface are shown.

**Supplementary Figure 2: Distribution of the residual interaction energies of the catalytic domain of FXa with the K2 domain of TFPI.**

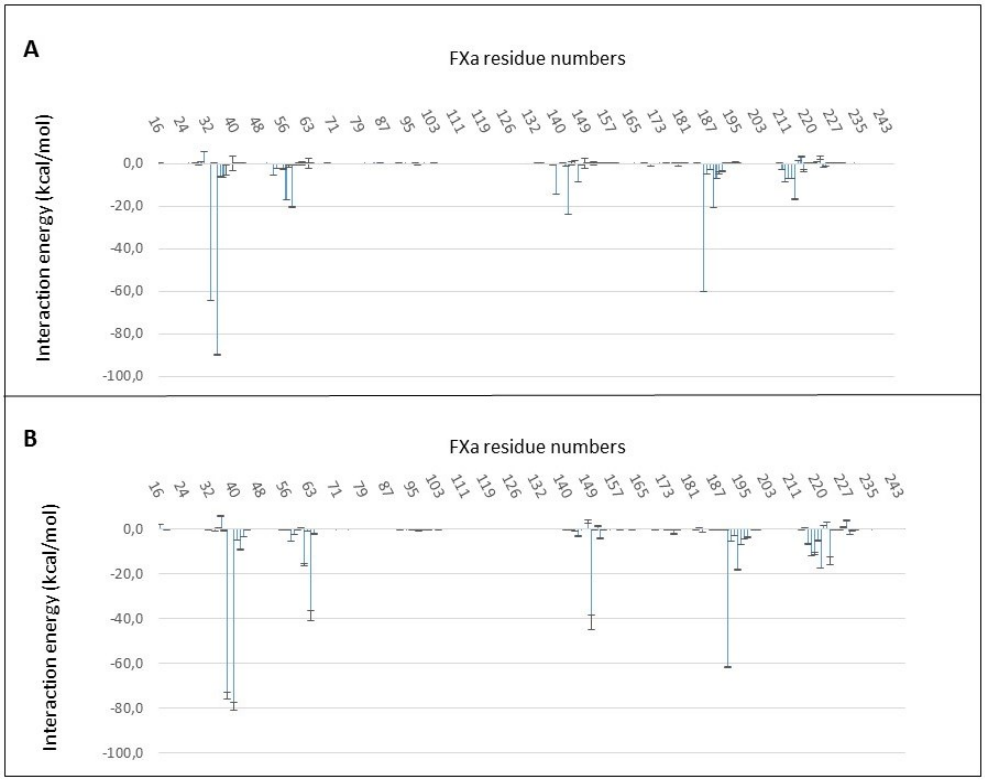


The plots are for wild-type GD-FXa (A) and S195A GD-FXa (B) catalytic domains residues.

**Supplementary Figure 3A: SDS-PAGE analysis of purified S195A GD-FXa**.

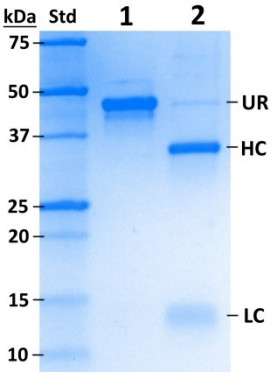


The protein was purified from the supernatant of drosophila S2 cells at day 6 post transfection as described in Methods. Under reducing conditions, the light chain that does not contain tryptophan is not visible on Stain Free gels (Biorad, data not shown). But as expected, the revelation with Coomassie Blue

confirmed the presence of the light chain. UR: unreduced, HC: heavy chain, LC: light chain, Std: protein molecular weight standards.

**Supplementary Figure 3B: Quality control of purified S195A GD-FXa by mass spectrometry.**

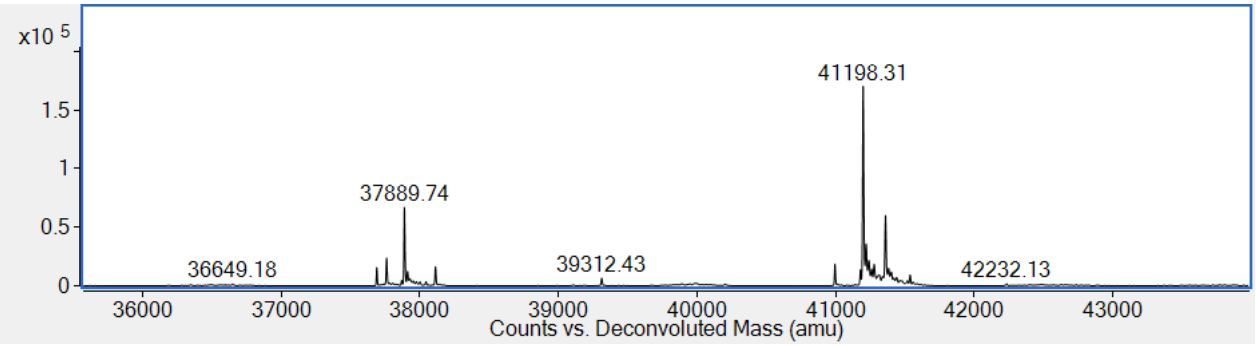


The sample was analyzed on a 6210 LC-ESI-TOF mass spectrometer (Agilent Technologies). The spectrum presented was obtained after deconvolution of the raw spectrum. The main peak at 41198 Da corresponds to the two chains linked by a disulfide bridge after cleavage by furin between the two chains with elimination of the peptide RKRRKR. The smaller peak 37889.74 may correspond to degradation of the protein.

## Supplementary references


1. Brooks BR, Bruccoleri RE, Olafson BD, States DJ, Swaminathan S, Karplus M. Charmm - a Program for Macromolecular Energy, Minimization, and Dynamics Calculations. Journal of Computational Chemistry. 1983;4(2):187-217.
2. Mackerell AD, Jr. Empirical force fields for biological macromolecules: overview and issues. J Comput Chem. 2004 Oct;25(13):1584-604.
3. Buck M, Bouguet-Bonnet S, Pastor RW, MacKerell AD, Jr. Importance of the CMAP correction to the CHARMM22 protein force field: dynamics of hen lysozyme. Biophys J. 2006 Feb 15;90(4):L36-8.
4. Jorgensen WL, Chandrasekhar J, Madura JD, Impey RW, Klein ML. Comparison of Simple Potential Functions for Simulating Liquid Water. Journal of Chemical Physics. 1983;79(2):926-35.
5. Feller SE, Zhang YH, Pastor RW, Brooks BR. Constant Pressure Molecular Dynamics Simulation: the Langevin Piston Method Journal of Chemical Physics. 1995 Feb 20;103(11):4613-21.
6. Ryckaert JP, Ciccotti G, Berendsen HJC. Numerical-Integration of Cartesian Equations of Motion of a System with Constraints - Molecular-Dynamics of N-Alkanes. Journal of Computational Physics. 1977;23(3):327-41.
7. Burgering MJ, Orbons LP, van der Doelen A, Mulders J, Theunissen HJ, Grootenhuis PD, et al. The second Kunitz domain of human tissue factor pathway inhibitor: cloning, structure determination and interaction with factor Xa. Journal of molecular biology. 1997 Jun 13;269(3):395-407.
8. Kollman PA, Massova I, Reyes C, Kuhn B, Huo S, Chong L, et al. Calculating structures and free energies of complex molecules: combining molecular mechanics and continuum models. Accounts of chemical research. 2000 Dec;33(12):889-97.
9. Nina M, Im W, Roux B. Optimized atomic radii for protein continuum electrostatics solvation forces. Biophysical chemistry. 1999 Apr 05;78(1-2):89-96.